Photophysical Properties of Lanthanide Dinuclear Complexes with *p-tert*-Butylcalix[8]arene[1,2]

Jean-Claude G. Bünzli,*,† Pascal Froidevaux,† and Jack M. Harrowfield‡

Institut de chimie minérale et analytique, Université de Lausanne, 3 Place du Château, CH-1005 Lausanne, Switzerland, and Department of Chemistry, University of Western Australia, Nedlands, WA, Australia

Received November 20, 1992

The macrocyclic octaphenol *p-tert*-butylcalix[8]arene (LH_8) was reacted with lanthanide(III) ions in dimethylformamide (DMF) containing triethylamine to obtain both homo- and heterodinuclear neutral complexes of composition $[(Ln1{:}Ln2)LH_2(DMF)_5](DMF)_n$, with $n = 4$ (α-phase) or 1.5 (β-phase). ICP-AES determination of the Ln(III) content shows a clear selectivity of the ligand for ions in the middle of the lanthanide series. Luminescence measurements at 77 K suggest that the two lanthanide(III) ions encompassed by the ligand are in very similar environments with *pseudo* C_{3h} symmetry. Small differences in the crystal-field potential are evidenced between the two crystalline phases and when a large ion (*e.g* Nd) is encapsulated by the ligand. The presence of a low-lying metal-to-ligand charge-transfer state (MLCT) in the Eu-containing complexes at *ca.* 20 000 cm^{-1} induces unusual spectroscopic properties. Very large absorption probabilities ($\sim 10^{-6}$) have been determined for the Eu(III) transitions, and the Judd–Ofelt theory for f–f transitions fails to explain the very large value of the Ω_2 parameter (448×10^{-20} cm^2). In DMF solution, an efficient energy transfer from the ligand to Tb(III) occurs and makes the Tb(III) calixarene complex an interesting luminescent label.

Introduction

Lanthanide luminescent probes are convenient tools to help in solving a variety of analytical and structural problems. In particular, they are presently extensively used for studying metal ion sites in macrocyclic complexes[3,4] and in biological systems.[4,5] In view of the long lifetimes of their excited states, Eu(III) and Tb(III) ions are especially suitable for the determination of metal ion distances in biological and macrocyclic systems[4-6] and of the number of water molecules bonded to lanthanide(III) ions.[4,5,7] The need for luminescent tags to develop more sensitive fluoroimmunoassays[5,8] or other clinical applications[8] has prompted the search for new lanthanide complexing agents. Potentially, macrocylic complexes offer access to the control of physical properties such as excited-state lifetimes or magnetism through variation of the ligand structure and rigidity. The present work is linked to our studies of the degree of control offered in complexes of the macrocyclic polyphenols known as the calixarenes.[9]

Calixarenes are a versatile class of macrocyclic molecules well suited to act as receptors for both neutral and cationic species. They are easy and cheap to synthesize by one-step procedures and combine good accessibility with a large variety of structures. The first complexes between calixarenes (Chart I) and lanthanide(III) ions have been reported by Harrowfield and co-workers, who isolated dinuclear complexes $[Ln_2LH_2(DMF)_5]\cdot n$DMF, where LH_2 stands for the hexaanion of *p-tert*-butylcalix[8]arene. The X-ray structure determination of the homodinuclear Eu complex with $n = 4$ (α-phase)[10] shows both Eu(III) ions encompassed by the ligand in essentially identical environments. The metal ions are 8-coordinate and bridged by two phenoxide donor atoms of the macrocyclic ligand and by a DMF molecule. Further complexes with Ln = La and Pr were characterized.[11a] A second phase ($n = 1.5$, β-phase) of dimethylformamide-solvated Eu[11b] and Lu[11a] complexes has been isolated and subjected to structural characterization. Despite substantial differences in the parameters of the crystallographic unit cell, the coordination polyhedron for Eu(III) is essentially identical in both phases. Other isolated complexes include $[Ln_2LH_2(DMSO)_5]\cdot n$DMSO, Ln = La, Eu, Tm, and Lu,[12a] $[EuLH_6(NO_3)(DMF)_4]\cdot 3DMF$,[12b] $[Eu(L^2H_4)(OH)(DMF)_6]\cdot L^2H_6\cdot 4DMF$ (L^2H_6 = *p-tert*-butylcalix-

Chart I

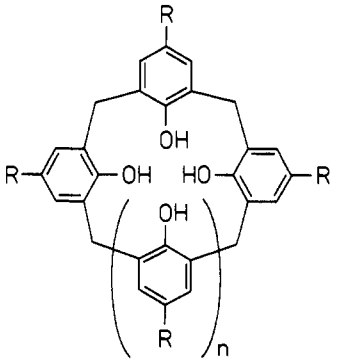

† University of Lausanne.
‡ University of Western Australia.

(1) Complexes of Lanthanoid Salts with Macrocyclic Ligands. 41. Part 40: Reference 3.
(2) Abstracted, in part, from the Ph.D. Thesis of P. Froidevaux, University of Lausanne, 1992.
(3) Moret, E.; Nicolò, F.; Plancherel, D.; Froidevaux, P.; Bünzli, J.-C. G. *Helv. Chim. Acta* **1991**, *74*, 65.
(4) Horrocks, W. de W., Jr.; Albin, M. *Prog. Inorg. Chem.* **1984**, *31*, 1.
(5) Bünzli, J.-C. G. In *Lanthanide Probes in Life, Chemical, and Earth Sciences. Theory and Practice*; Bünzli, J.-C. G., Choppin, G. R., Eds.; Elsevier Science Publ.: Amsterdam, 1989; Chapter 7.
(6) Guerriero, P.; Vigato, P. A.; Bünzli, J.-C. G.; Moret, E. *J. Chem. Soc., Dalton Trans.* **1990**, 647.
(7) Moret, E.; Bünzli, J.-C. G.; Schenk, K. J. *Inorg. Chim. Acta* **1990**, *178*, 83.
(8) Evans, C. H. *Biochemistry of the Lanthanides*; Plenum Press: New York, 1990.
(9) (a) Gutsche, C. D. *Calixarenes*; Monographs in Supramolecular Chemistry; Stoddart, J. F., Ed.; Royal Society of Chemistry: Cambridge, U.K., 1989. (b) Bünzli, J.-C. G.; Harrowfield, J. M. In *Calixarenes: A Versatile Class of Macrocyclic Compounds*; Vicens, J., Böhmer, V., Eds.; Kluwer Academic Publ.: Dordrecht, The Netherlands, 1991.
(10) Furphy, B. M.; Harrowfield, J. M.; Kepert, D. L.; Skelton, B. W.; White, A. H. *Inorg. Chem.* **1987**, *26*, 4231.
(11) (a) Harrowfield, J. M.; Ogden, M. I.; White, A. H. *Aust. J. Chem.* **1991**, *44*, 1249. (b) Harrowfield, J. M.; Ogden, M. L.; White, A. H.; Wilner, F. R. *Aust. J. Chem.* **1989**, *42*, 949.

0020-1669/93/1332-3306$04.00/0

[6]arene),[13] $[Eu_2(L^3H)_2(DMF)_4]$ (L^3H_4 = *p-tert*-butylcalix[4]-arene),[14a] and the triple inclusion complex $[Eu_2(L^4H)_2(DMSO)_2]\cdot 2Me_2CO$ (L^4H_4 = bis(homooxa)-*p-tert*-butylcalix-[4]arene).[14b] Further, Sabbatini and co-workers[15] have reported a photophysical study of Eu(III) and Tb(III) complexes with a *p-tert*-butylcalix[4]arene tetraamide ligand. These compounds are water soluble and display interesting luminescent properties.

In this paper, we report a chemical and photophysical study of the dinuclear complexes $[(Ln^1_xLn^2_{2-x})LH_2(DMF)_5](DMF)_n$ with x = 2–0 and Ln = Nd, Eu, Tb, Gd, Ho, and Yb. We aim at probing the structural and luminescent properties of lanthanide-(III) ions held at a short distance (ca. 3.7 Å) in a macrocyclic ligand. Moreover, we determine the influence of a very low-lying charge-transfer state (LMCT) on the spectroscopic properties of Eu(III) and we assess the potential of calixarene complexes as spectroscopic labels.

Experimental Section

Preparation of the Crystalline Complexes. Ln(III) oxides (99.99%) were purchased from Glucydur, and all the other products, from Fluka (*puriss* quality). The ligand *p-tert*-butylcalix[8]arene (LH_8)[16] and the $Ln(NO_3)_3(DMSO)_n$ solvates[17] were synthesized according to literature methods. Purity of the ligand was controlled by TLC (hexane:$CHCl_3$ 4:3) and IR and ^{1}H-NMR spectra, which agreed with published data.[16] The homodinuclear complexes were synthesized as previously described.[10,11a] though the original method[10] was less preferred because several recrystallisations were required simply to ensure the complexes were completely free of DMSO. The doped complexes were obtained by adding a DMF solution containing Ln^1 and Ln^2 in the desired ratio to a DMF solution of the deprotonated ligand maintained at 60 °C. The complexes were recrystallized twice in DMF. The large crystals (*ca.* 2.5/2.5/0.5 mm) used in the luminescence study were obtained by cooling DMF solutions of the dry complexes (300 mg in 10 mL) stepwise from 100 to 40 °C during 3 days.

Physicochemical Measurements. The Ln content of the complexes was determined by ICP–AES (Perkin-Elmer 6600 ICP spectrophotometer). The samples were prepared by dissolving 30 mg of the dry complex in 10 mL of trichloroethylene (TCE, Fluka, pa); 20 mL of water acidified with concentrated $HClO_4$ (1 mL) was added, and the heterogeneous solution was vigorously stirred during 10 min. The aqueous phase was removed, diluted to 100 mL, and analyzed. The total Ln(III) content was around 40 mg/L. Standards were prepared from $LnCl_3$ solutions (1 g/L) in acidified water (Alfa Products). The following emission lines were used to perform the quantitative analyses: 410.946 nm (Nd), 342.247 nm (Gd), 381.967 nm (Eu), 350.917 nm (Tb), 345.600 nm (Ho), and 328.937 nm (Yb). Results are listed in Table I.

The IR spectra (KBr or polyethylene pellets) were recorded between 4000 and 100 cm^{-1} by use of a Bruker IFS-113v FT-IR or a Mattson Alpha Centauri spectrometer. Raman spectra between 100 and 3000 cm^{-1} (Ramalog-4, DM-3000 software from Spex Industries) were measured on small crystals introduced in capillary tube containing DMF. UV–vis absorption spectra were measured from TCE or DMF solutions in 1, 5, or 10 cm long quartz cells (Hellma-111 QS), using a Perkin-Elmer Lambda-7 or Lambda 19 spectrophotometer. Oscillator strengths (P) were calculated using Judd and Ofelt's definition:[18]

$$P = (2303mc^2/N\pi e^2)(9n/(n^2+2)^2)\int \epsilon_i(\nu)\, d\nu \qquad (1)$$

Absorbances were measured on large crystals introduced into a Pyrex tube (ϕ 5 mm) containing DMF. This tube was placed into a 1-cm cell (Hellma-111 QS), and the rotation of the tube allowed measurements according to the different axes of the crystals.

Luminescence measurements involving the singlet and triplet excited states of the ligand were performed using a Perkin-Elmer LS-50 spectrofluorometer. The solutions were deoxygenated by repeated vacuum–argon purge cycles and measured in 1-cm cells (Hellma-111 QS). Low-temperature experiments (77 K) on microcrystalline powders were performed using the No. L22500136 LS-50 accessory. The experimental procedures for Eu(III) and Tb(III) luminescence measurements have been previously published.[6,19] Intensities of the emission bands have been corrected for the instrumental response. To avoid desolvation of the complexes and to minimize the reflection of the incident excitation light, measurements were performed on large crystals (2.5 × 2.5 × 0.5 mm) immersed in a DMF-filled Pyrex tube (ϕ 5 mm) fixed onto an orientable support held in an Oxford DN 704 cryostat (77 K) or in an Oxford CF-204 (4.2 K) cryostat. Laser excitation light was focused on the crystal through a set of lenses placed on an orientable optical rail. Excitation of the Ln(III) ions was achieved through either the $^5D_0$(Eu) or the $^5D_4$(Tb) levels by means of a continuous dye laser (Rhodamine 6G) or a pulsed dye laser (Coumarine C102 or Rhodamine 6G).

Table I. Lanthanide(III) Ions Ratio in the Dinuclear Complexes $[(Ln^1_xLn_{2-x}^2)LH_2(DMF_5)]\cdot n$DMF As Weighed and Determined by ICP–AES

	% weighed[a]		% found[b]			% weighed[a]		% found[b]	
Ln^1–Ln^2	Ln^1	Ln^2	Ln^1	Ln^2	Ln^1–Ln^2	Ln^1	Ln^2	Ln^1	Ln^2
Eu–Nd	95	5	98	2	Eu–Gd	2	98	2	98
	90	10	97	3		10	90	12	88
	50	50	74	26		12	88	14	86
	10	90	19	81		20	80	24	76
	5	95	11	89		50	50	57	43
						90	10	94	6
Tb–Nd	10	90	16	84	Tb–Gd	5	95	7	93
	5	95	6	94		15	85	19	81
	50	50	74	26		50	50	59	41
						85	15	89	11
Eu–Tb	90	10	91	9		95	5	97	3
Eu–Nd[c]	95	5	98	2	Tb–Ho	50	50	54	46
	90	10	96	4		75	25	77	23
	80	20	94	6					
	50	50	72	28	Eu–Yb	10	90	33	66

[a] Introduced into the synthesis mixture. [b] After two recrystallizations in DMF. [c] Measured on a large single crystal used for the luminescence experiments.

Results and Discussion

Complex Formation. The reaction of *p-tert*-butylcalix[8]arene (LH_8) with 2 equiv of $Ln(NO_3)_3(DMSO)_n$ and 6 equiv of triethylamine in DMF yields a 2:1 crystalline adduct.[10] Complex formation is particularly noticeable in the case of Eu(III), the solution becoming instantaneously orange. This is related to the presence of a low-energy ligand-to-metal charge-transfer state (LMCT) lying at 25 640 cm^{-1}. The identification of the LMCT state in crystals is more complicated, due to preferential absorptions along the different axes of the crystals and to the stacking of the phenolic units, likewise evidenced in the *p-tert*-butylcalix[4]arene tetraamide complex with Eu(III).[15a] Absorbance and reflectance experiments on crystals show that the geometry of the samples has a considerable influence on the shape and position of the LMCT absorption (*cf.* Figure S1, supplementary material). For instance, we observe a large bathochromic shift in the crystals and the broad LMCT band is centered at 20 000 cm^{-1}. Complex formation is further evidenced by IR and Raman spectra, which display a large drop in the ν(O–H) band intensity at 3000–3600 cm^{-1}. Simultaneously, a weak band appears at 160–170 cm^{-1}, which we assign to a metal–oxygen

(12) (a) Harrowfield, J. M.; Ogden, M. I.; White, A. H. *Aust. J. Chem.* **1991**, *44*, 1237. (b) Harrowfield, J. M.; Ogden, M. I.; Richmond, W. R.; White, A. H. *J. Chem. Soc., Dalton Trans.* **1991**, 2153.
(13) Engelhardt, L. M.; Furphy, B. M.; Harrowfield, J. M.; Kepert, D. L.; White, A. H.; Wilner, F. R. *Aust. J. Chem.* **1988**, *41*, 1465.
(14) (a) Furphy, B. M.; Harrowfield, J. M.; Ogden, M. I.; Skelton, B. W.; White, A. H.; Wilner, F. R. *J. Chem. Soc., Dalton Trans.* **1989**, 2217. (b) Asfari, Z.; Harrowfield, J. M.; Ogden, M. I.; Vicens, J.; White, A. H. *Angew. Chem., Int. Ed. Engl.* **1991**, *30*, 854.
(15) (a) Hazenkamp, M. F.; Blasse, G.; Sabbatini, N.; Ungaro, R. *Inorg. Chim. Acta* **1990**, *172*, 93. (b) Sabbatini, N.; Guardigli, N.; Mecati, A.; Balzani, V.; Ungaro, R.; Ghidini, E.; Casnati, A.; Pochini, A. *J. Chem. Soc., Chem. Commun.* **1990**, 878.
(16) Gutsche, C. D.; Dhawan, B.; No, K. H.; Muthukrishnan, R. *J. Am. Chem. Soc.* **1981**, *103*, 3782.
(17) Ramaligam, S. K.; Soundararajan, S. *J. Inorg. Nucl. Chem.* **1967**, *29*, 1763.
(18) Carnall, W. T.; Fields, P. R.; Rajnak, R. *J. Chem. Phys.* **1968**, *49*, 4412.
(19) Bünzli, J. C. G.; Pradervand, G. O. *J. Chem. Phys.* **1986**, *85*, 2489. Bünzli, J. C. G.; Plancherel, D.; Pradervand, G. O. *J. Phys. Chem.* **1989**, *93*, 980.

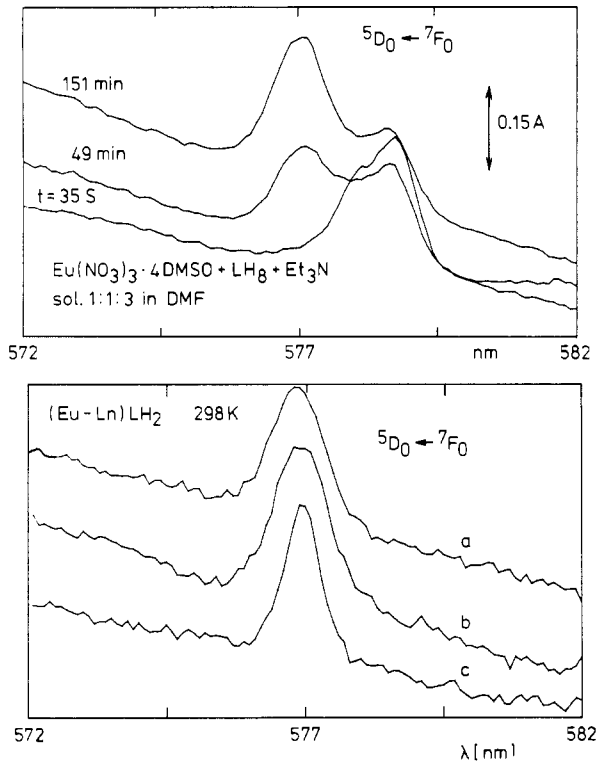

Figure 1. Absorption spectra of the $^5D_0 \leftarrow {}^7F_0$ transition in $[Eu_2(LH_2)(DMF)_5]\cdot 4DMF$. Top: Mono- and dinuclear complex formation as a function of time. Bottom: Crystals in solution in (a) DMF and (b) TCE and (c) large single crystal.

vibration. Furthermore, a new band at 1650 cm^{-1} corresponds to the ν(C=O) mode of DMF molecules bonded to the Ln(III) ion.

In the case of the Eu(III) dinuclear complexes, the presence of the LMCT state drastically relaxes the Laporte's rule so that the usually nonnoticeable $^5D_0 \leftarrow {}^7F_0$ absorption can be easily detected in the UV–visible absorption spectra. Immediately after mixing of the reactants, one band is observed at 17 274 cm^{-1}, assigned to an absorption from a mononuclear species. This band progressively disappears and is replaced by the absorption of the dinuclear species at 17 330 cm^{-1}. Dissolution of the crystalline dinuclear complex in trichloroethylene (TCE) or DMF or direct absorption measurements on a large crystal of $[Eu_2LH_2(DMF)_5]\cdot 4DMF$ result in spectra displaying only one $^5D_0 \leftarrow {}^7F_0$ band at 17 330 cm^{-1}. This points to the exclusive presence of the most stable dinuclear species in solution (Figure 1).

From the ICP–AES analyses reported in Table I it is clear that *p-tert*-butylcalix[8]arene forms preferentially crystalline complexes with cations in the middle of the lanthanide series. We have also found that large crystals of both α- and β-phases can be grown if a larger ion such Nd(III) is added. The only other system crystallizing within both phases is $[(Eu_{0.04}Gd_{1.96})LH_2(DMF)_5]\cdot n DMF$. Therefore, larger ions seems to favor the β-phase while smaller lanthanides induce a preferential crystallization in the α-phase.

Luminescence of the Complexes. The synthetic method used for the doped complexes leads to a distribution of the two homodinuclear and of the heterodinuclear species: Ln^1Ln^1, Ln^2Ln^2, and Ln^1Ln^2. This is confirmed by lifetime measurements of the $^5D_0$(Eu) excited state. The Eu homodinuclear complex displays a mono-exponential decay (78 μs), while a two-exponential decay is observed for $[(Eu_xLn_{2-x})LH_2(DMF)_5]\cdot 4DMF$ heterodinuclear complexes (Ln = Gd, Tb; 64 and 150 μs); these data will be discussed separately.[20] Whenever necessary, interpretation of physicochemical measurements has consequently been done by assuming a statistical 1:1:2 distribution of these species in the compounds. The data of Table I show this assumption to be correct, at least for the intermediate Ln(III) ions.

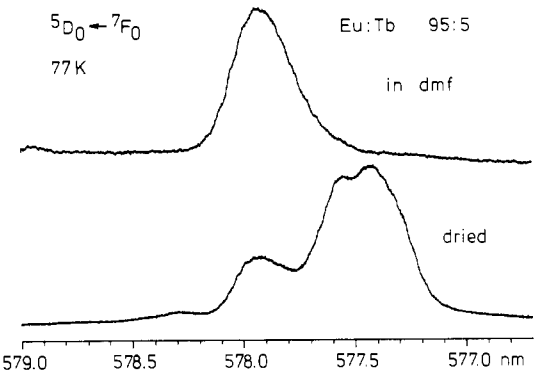

Figure 2. Excitation spectra of the $^5D_0 \leftarrow {}^7F_0$ transition in $[(Eu_{0.1}Tb_{1.9})(LH_2)(DMF)_5]\cdot 4DMF$. λ_{an} = 617.5 nm. Top: Crystal in a DMF-filled tube. Bottom: Microcrystalline powder dried over P_2O_5 and 10^{-2} Torr.

The luminescent properties of Eu(III) ions encapsulated in *p-tert*-butylcalix[8]arene are subordinated to the quenching effect of the low-lying LMCT state. Therefore, we observe only a very weak emission from the $^5D_0$(Eu) level at room temperature, a weak emission at 77 K, and a somewhat more intense emission at 4.2 K. The strong temperature dependence of the Eu(III) emission intensity is observed in all the Eu-containing complexes (cf. Figure S2, supplementary material). In the case of the EuNd heterodinuclear complex, an efficient Eu → Nd energy transfer further quenches the Eu luminescence.

Ligand and LMCT absorptions are not observed in the Eu(III) excitation spectra because of efficient nonradiative processes arising from the mixing of the LMCT state with the ^{7}F(Eu) configuration. If the LMCT state lies at higher energy, the mixing is considerably reduced: both ligand and LMCT bands were identified in dilute solutions of the *p-tert*-butylcalix[4]arenetetraamide complex with Eu (LMCT: 29 400 cm^{-1}).[15] A schematic configurational coordinate diagram model[21] shows that the LMCT excited state can directly feed the ground ^{7}F manifold at room temperature, bypassing the luminescent ^{5}D levels. In the crystalline and glass forms of GdB_3O_6:Eu^{3+}, Blasse[22] evidences very different quantum efficiencies of the luminescence upon LMCT excitation due to the larger equilibrium distance for the looser glass structure. This example proves that a larger LMCT parabola offset results in a direct feeding of the ground ^{7}F levels.

In both α- and β-phases, the nondegenerate $^5D_0 \leftarrow {}^7F_0$ transition is comprised of a single broad band (fwhh between 9 and 13 cm^{-1}), at 17 297 ± 1 cm^{-1} in α-crystals and slightly blue shifted at 17 300 cm^{-1} in β-crystals. A very weak absorption is also visible at ~17 318 cm^{-1} on the $^5D_0$(Eu) excitation spectra and is assigned to a desolvated species becoming predominant upon drying the crystals in a desiccator (Figure 2). We conclude that the two Ln(III) ion sites are very similar in each crystalline phase for all the studied complexes.

Selective excitations at 77 and 4.2 K in the region of the $^5D_0 \leftarrow {}^7F_0$ transition yield emission spectra having the same shape for all the doped series of α-crystals, pointing to isostructural complexes (Figure 3). The same experiments on β-crystals reveal slight differences between $[(Eu_{0.04}Gd_{1.96})LH_2(DMF)_5]\cdot 1.5DMF$ and $[(Eu_xNd_{2-x})LH_2(DMF)_5]\cdot 1.5DMF$, x = 1.9 and 1.8, probably due to the difference in the ionic radii of Gd and Nd. However, the most noticeable differences occur between the two phases, as shown in Figure 4; ^7F_j levels are listed in Tables IV and S1 (supplementary material) for some typical complexes.

The isolation of two different crystalline phases allows us to consider the effect of two slightly different crystal fields on the

(20) Froidevaux, P.; Bünzli, J.-C. G. Submitted for publication.

(21) Struck, C. W.; Fonger, W. H. *J. Chem. Phys.* **1970**, *52*, 6364.
(22) Blasse, G. *Mater. Chem. Phys.* **1992**, *31*, 3.

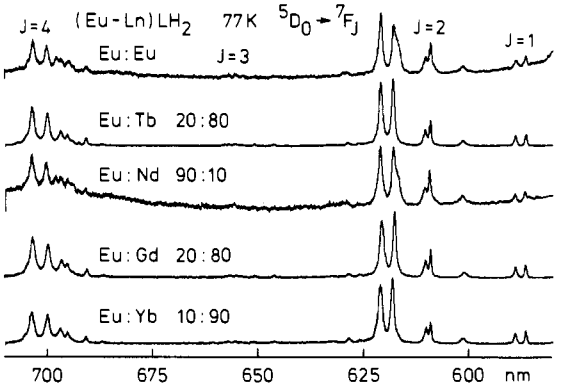

Figure 3. Part of the emission spectrum of the $^5D_0$(Eu) level in $[(Eu_xLn_{2-x})(LH_2)(DMF)_5]\cdot 4DMF$. λ_{exc} = maximum of the $^5D_0 \leftarrow {}^7F_0$ transition.

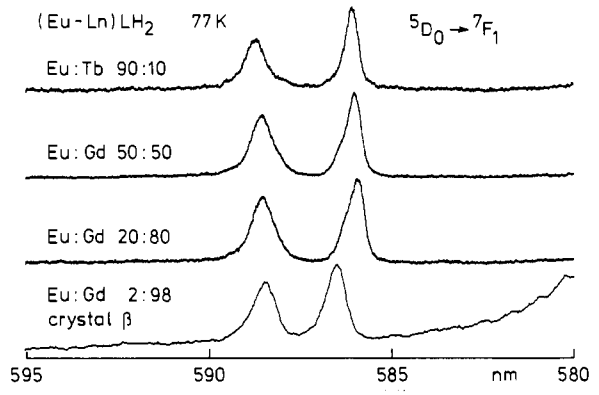

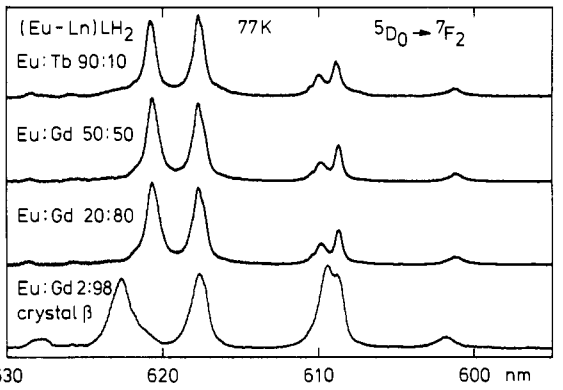

Figure 4. Emission of the $^5D_0 \rightarrow {}^7F_1$ (top) and $^5D_0 \rightarrow {}^7F_2$ (bottom) transitions in $[(Eu_xLn_{2-x})(LH_2)(DMF)_5]\cdot n$DMF in crystals of the α-phase (top three spectra) and β-phase (bottom spectrum). λ_{exc} = maximum of the $^5D_0 \leftarrow {}^7F_0$ transition.

same idealized symmetry. The crystal-field splittings at 77 K of the $^5D_0 \rightarrow {}^7F_1$ transition in $[(Eu_xLn_{2-x})LH_2(DMF)_5]\cdot n$DMF in both phases (Figure 5, top) display evidence for a pseudo-trigonal symmetry.[9b] The splitting of 45 cm^{-1} between the two components (A′ + E″) of the transition in the β-crystal $[(Eu_{0.04}Gd_{1.96})LH_2(DMF)_5]\cdot 1.5$DMF is similar to the splittings measured for Eu(III) ethyl sulfates and triflates in a C_{3h} symmetry, 38 and 44 cm^{-1}, respectively.[23]

The relative intensities of the $^5D_0 \rightarrow {}^7F_J$ transitions reported in Table II show the predominance of the hypersensitive $^5D_0 \rightarrow {}^7F_2$ transition. This points to a less symmetrical ion site polyhedron than the idealized trigonal symmetry. In a previous study of 4:3 complexes with 18-crown-6 ether,[19] we have shown that a small deviation from an idealized coordination polyhedron dramatically affects the intensity of the electric dipole $^5D_0 \rightarrow {}^7F_2$ transition. Moreover, the presence of the low-lying LMCT increases

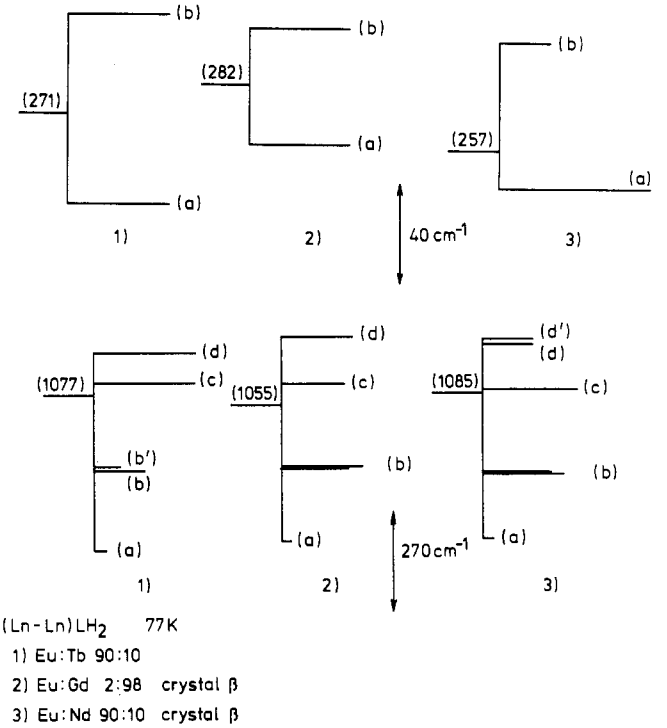

Figure 5. Crystal field splittings of the $^7F_1$ (top) and $^7F_2$ (bottom) levels identified in $[(Eu_xLn_{2-x})(LH_2)(DMF)_5]\cdot 4$DMF at 77 K.

Table II. Corrected Intensities Relative to $^5D_0 \rightarrow {}^7F_1$ of the $^5D_0 \rightarrow {}^7F_J$ Transitions in Single Crystals of the Complexes $[(Eu_xLn_{2-x})LH_2(DMF)_5]\cdot 4$DMF ($\alpha$-phase; λ_{exc} = Maximum of the $^5D_0 \leftarrow {}^7F_0$ Band)

J	$Eu_{0.2}Gd_{1.8}$	$Eu_{0.4}Gd_{1.6}$	$Eu_{1.0}Gd_{1.0}$	$Eu_{1.8}Gd_{0.2}$	$Eu_{1.8}Tb_{0.2}$	$Eu_{1.0}Eu_{1.0}$
1	1.0	1.0	1.0	1.0	1.0	1.0
2	11.8	10.8	12.2	12.4	12.6	17.0
3	0.2	0.56	0.55	0.55	0.8	0.55
4	10.3	8.7	9.9	11.0	9.9	10.1

Table III. Corrected Intensity R of the Transitions $^5D_0 \rightarrow {}^7F_2$ Relative to the Magnetic Dipole $^5D_0 \rightarrow {}^7F_1$ in Compounds Doped by Eu(III) and Energy of the LMCT State[24]

compd	$R \pm$ 10%	LMCT (10^3 cm^{-1})	compd	$R \pm$ 10%	LMCT (10^3 cm^{-1})
$ScPO_4:Eu^{3+}$	1.6	48.0	$ScVO_4:Eu^{3+}$	8.4	29.8
$YPO_4:Eu^{3+}$	2.3	45.0	$[Eu_2LH_2(DMF)_5]\cdot 4$DMF[a]	17.0	20.0
$YVO_4:Eu^{3+}$	6.5	31.2			

[a] This work; crystal in DMF.

considerably the hypersensitivity of the electric dipolar transitions. A correlation between the position of the LMCT and the intensity of the electric dipolar transitions has been unraveled by Blasse[24] (see Table III). The crystal-field splittings of the $^7F_2$ levels are displayed in Figure 5 and Table IV. To discuss these splittings, we start from the idealized C_{3h} symmetry for which two components of the magnetic dipole transition $^5D_0 \rightarrow {}^7F_1$ are allowed (A′ → A′, A′ → E″) as well as three components of the $^5D_0 \rightarrow {}^7F_2$ transition: A′ → E′, electric dipole; A′ → A′ and A′ → E″, magnetic dipole.[5] We then evaluate how the E′ and E″ levels are split by the lowering of the symmetry in α- and β-crystals. For $^7F_2$ we observe three main groups of components b–d in addition to a vibronic component a at 670 cm^{-1} from the ground level arising from the activation of a ν(DMF) vibration (IR, 662 cm^{-1}; Raman, 664 cm^{-1}). Component c is assigned to the A′ → A′ transition because no change at all in its shape and energy occurs for all the investigated complexes, indicating no crystal-field effect. The latter split component b into b and b′ for all the complexes, but the splitting is less important in β-crystals than in α-crystals. We assign the corresponding transition to A′ →

(23) Moret, E.; Nicolò, F.; Bünzli, J.-C. G.; Chapuis, G. *J. Less-Common Met.* **1991**, 273.

(24) Blasse, G.; Bril, A. *J. Chem. Phys.* **1969**, *50*, 2974.

Table IV. Identified Crystal Field Levels (in cm^{-1} from $^7F_0$) in $[(Eu_xLn_{2-x})LH_2(DMF)_5]\cdot n$DMF at 77 K

level	$Eu_{1.0}Eu_{1.0}$- (α-phase)	$Eu_{1.8}Nd_{0.2}$- (β-phase)	$Eu_{0.04}Gd_{1.98}$- (β-phase)
$^7F_0$	0	0	0
$^7F_1$	238	243	249
	306	295	305
$^7F_2$	872	862	873
	901	884	889
	1113	1102	1106
	1184	1198	1237
		1230	
$^7F_4$	2813	2834	2829
	2905	2913	2907
	2941	2969	2969
	3003	3020	3013
	3079	3078	3068
		3116	3116

E′ (or E″). On the other hand component d is not split by crystal-field effects in α- and β-crystals but the introduction of Nd(III) ions creates another perturbation in β-crystals that splits this component into d and d′; therefore, we assign this component to the second A′ → E″ (or E′) transition allowed in C_{3h} symmetry. From this analysis, we conclude that the coordination polyhedron of Eu(III) in the two crystalline phases of $[(Eu_xLn_{2-x})LH_2(DMF)_5]\cdot n$DMF complexes effectively displays the trace of a pseudo-C_{3h} symmetry. The observation of five components only for the $^5D_0 \rightarrow {}^7F_4$ transition is consistent with the latter symmetry.

In order to confirm the isostructural nature of the complexes when a lanthanide ion is replaced by another one, the Tb($^5D_4$) luminescence has been recorded upon excitation of the $^5D_4 \leftarrow {}^7F_6$ transition at 482 nm. The $^5D_4 \rightarrow {}^7F_J$ (J = 5, 4, 3) transitions display no modification in Eu(III), Gd(III), Ho(III), and Nd(III) complexes doped with varying percentages of Tb(III). The spectra are dominated by the $^5D_4 \rightarrow {}^7F_5$ transition (Figure S3, supplementary material). Efficient energy transfer from Tb(III) to Eu(III), Nd(III), and Ho(III) is evidenced by the large decrease in luminescence intensity when the concentration of Eu(III), Ho(III), and Nd(III) is increased, while the Tb-doped series of complexes displays no evidence for a concentration quenching.

Photophysical Study. One of the reasons we are investigating lanthanide complexes with calixarenes is to find out whether or not they display an efficient antenna effect. We have studied the lanthanide ion and ligand absorption and luminescent properties in both the homo and heterodinuclear complexes. A special attention was devoted to the various energy-transfer processes taking place in these compounds.

A noteworthy finding is the unusually high energies at which the f–f absorption transitions are observed. The $^5D_0 \leftarrow {}^7F_0$ transition occurs at $\tilde{\nu}$ = 17 298 cm^{-1}, a value out of the range of the correlation proposed by Horrocks[25] between the energy of this transition and the formal total charge of the ligands bonded to Eu(III). Moreover, a frequency of about 20 750 cm^{-1} for the $^5D_4 \leftarrow {}^7F_6$ transition of the Tb(III) ion is 100–200 cm^{-1} higher than for the aquo ion[5] and the $^2F_{7/2} \leftarrow {}^2F_{5/2}$ transition of the Yb(III) ion appears in a spectral region between 10 200 and 11 400 cm^{-1} ($YbCl_3$: 9400–11 300 cm^{-1}). We interpret these data as evidence for a ligand–metal bond having sizable covalent character, due to a high polarizability of the ligand. This explanation is substantiated by the calculated electronegativity of the ligand. Taking 1.9 as the electronegativity of the Eu(III) ion,[26] we find $\chi_{opt}(LH_2)$ = 2.6 for the complex in solution, a value lower than the range observed for crown ethers, 2.7–3.0.[27] Using the same value for χ_{opt}(Eu) and the data published by Blasse and Sabbatini,[15] we determine a χ_{opt}(L) value of 2.9 for the *p-tert*-butylcalix[4]arene tetraamide in which the donor oxygen atoms are not phenolic. Therefore, *p-tert*-butylcalix[8]arene can be considered as a better electron donor ligand.

Moreover, unusually large absorption probabilities are observed for the f–f transitions in the Eu-containing complexes. The calculated probabilities (eq 1) are 0.63×10^{-6} for $^5D_0 \leftarrow F_0$, 1.25×10^{-6} for $^5D_1 \leftarrow {}^7F_0$, and 10.6×10^{-6} for $^5D_2 \leftarrow F_0$. The usual range of P-values for lanthanide ions is 10^{-8}–10^{-9}.[18] Within the Judd–Ofelt formalism,[28,29] the Ω_2 parameter only can be calculated, the $\langle U^{(\lambda)} \rangle$ matrix elements vanishing for λ = 0 and 1. Using the $\langle U^{(\lambda)} \rangle$ data tabulated by Carnall et al.,[30] we calculate a value of 448×10^{-20} cm^2 for Ω_2, as compared to the (0.1–10) $\times 10^{-20}$ cm^2 usually reported for lanthanide ions.[26,31] This means that the $\langle U^{(\lambda)} \rangle$ matrix elements are not valid for $[(Eu_xLn_{2-x})LH_2(DMF)_5]\cdot n$DMF. Indeed no interaction between the ground 4f configuration and the excited LMCT or $4f^{n-1}5d^1$ configurations is taken into account. In Eu-containing compounds, the low-lying LMCT state interacts substantially with the ^{7}F(Eu) configuration[33,34] invalidating the assumptions upon which the Judd–Ofelt theory is based. In particular, the high absorption probabilities for the $^5D_{0,1,2} \leftarrow {}^7F_0$ transitions point to nonzero values for the corresponding $\langle U^{(\lambda)} \rangle$ matrix elements.

Hoshina et al. have investigated the effects of LMCT states on the Eu(III) luminescent properties.[33] Assuming that the mixing of the LMCT state with the ^7F_J levels enhances the equilibrium distance of the latter within the schematic configurational coordinate diagram model, they conclude that the fwhh of absorption bands should increase with the Eu(III) concentration, in comparison with the emission bands of the nonperturbed ^5D_J levels. In our compounds, an increase of the Eu(III) concentration from 10 to 100% induces an increase in the fwhh from 9 to 13 cm^{-1} while the width of the emission bands remains constant (Figure S4, supplementary material).

Intramolecular Ligand-to-Metal Energy Transfer. Encapsulation of Eu(III) and Tb(III) ions in suitable ligands is known to yield highly luminescent species which can be used as probes for a variety of applications;[15b] *p-tert*-butylcalix[8]arene contains eight phenolic units which can act as antenna for light absorption through a $\pi \rightarrow \pi^*$ transition. Due to the large molar absorption coefficient of the latter, subsequent excitation of Ln(III) by intramolecular ligand-to-metal energy transfer yields highly luminescent compounds.[35] Therefore, an efficient ligand-to-metal energy transfer implies an important overlap of the ligand and metal orbitals so that few complexes present a very high Ln(III) emission yield through ligand excitation. We have found that the Tb(III) complex with *p-tert*-butylcalix[8]arene exhibits strong luminescent properties upon ligand excitation. In DMF solutions, the detection limit for the Tb(III) emission is 10^{-10} M. The $^1(\pi\pi^*)$ emission of the ligand is easily detected in solutions and microcrystalline powders at 298 K. Moreover, one clearly evidences a broad $^3(\pi\pi^*)$ ligand phosphorescence by time-resolved spectroscopy on microcrystalline powders at 77 K. The ligand emission is particularly concentration sensitive and begins to decrease for solutions 5×10^{-4} M. In the solid state, Tb(III) excitation spectra display only a weak ligand absorption (Figure

(25) Albin, M.; Horrocks, Jr., W. de W., Jr. *Inorg. Chem.* **1985**, *24*, 895.
(26) Reisfeld, R.; Jørgensen, C. K. *Lasers and Excited States of Rare Earths*; Springer Verlag: Berlin, 1977.
(27) Bünzli, J.-C. G. In *Handbook on the Physics and Chemistry of Rare Earths*; Gschneidner, K. A., Eyring, L., Eds.; North-Holland: Amsterdam, 1987; Vol. 9, Chapter 60.
(28) Judd, B. R. *Phys. Rev.* **1962**, *127* (3), 750.
(29) Ofelt, G. S. *J. Chem. Phys.* **1962**, *37* (3), 511.
(30) Carnall, W. T.; Fields, P. R.; Rajnak, K. *J. Chem. Phys.* **1968**, *49* (10), 4450.
(31) J-mixing may also enhance transition probabilities but not to this extent.[32]
(32) Porcher, P.; Caro, P. *J. Chem. Phys.* **1978**, *68* (9), 4177.
(33) Hoshina, T.; Imanaga, S.; Yokono, S. *J. Lumin.* **1977**, *15*, 455.
(34) Judd, B. R. *J. Phys. C: Solid State Phys.* **1980**, *13*, 2695.
(35) Alpha, B.; Ballardini, R.; Balzani, V.; Lehn, J.-M.; Perathoner, S.; Sabbatini, N. *Photochem. Photobiol.* **1990**, *52*, 299.

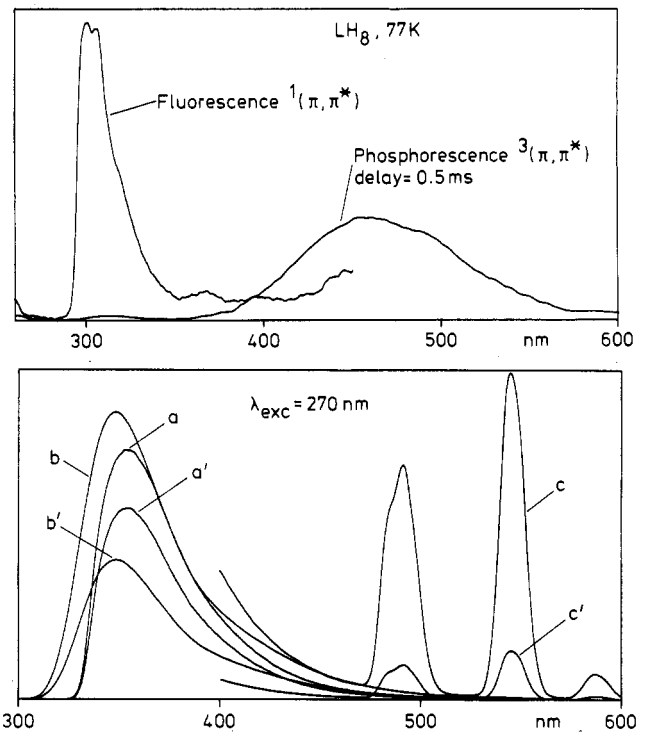

Figure 6. Top: Fluorescence and phosphorescence of a microcrystalline powder of the ligand LH_8. Bottom: Emission spectra of solutions of complexes in DMF at 298 K under ligand excitation. Key: (a) $[Yb_2(LH_2)(DMF)_5]\cdot 4DMF$; (b) LH_8; (c) $[Tb_2(LH_2)(DMF)_5]\cdot 4DMF$. The index (′) refers to solutions saturated with oxygen.

S3, supplementary material). Therefore, the rate of the energy migration through the crystal until a killer site is reached is larger than the rate of the intramolecular energy transfer. Blasse and Sabbatini[15] have observed similar features in the complex of *p-tert*-butylcalix[4]arene tetraamide with Eu(III). These authors attribute the large rate of energy migration to intermolecular interactions between arene units in the crystal, which disappear in solution.

The ligand phosphorescence covers the 400–500-nm spectral range resulting in a good resonance between the $^3(\pi\pi^*)$ state and the $^5D_4$(Tb) level. Therefore, an efficient energy-transfer process takes place from the ligand to the Tb(III) ion. The participation of the $^3(\pi\pi^*)$ level to the energy conversion is established through observation of a bimolecular oxygen triplet quenching of the Tb(III) luminescence upon ligand excitation (Figure 6). The long-lived $^3(\pi\pi^*)$ excited level interacts in a reversible way with oxygen molecules present in the solution. It is well demonstrated that the energy transfer from the ligand to the metal takes place through an exchange interaction[36] originating from the overlap of the electronic clouds of the atoms participating in the metal–ligand bond. In the same way, we have also evidenced a back-transfer from the $^5D_3$(Tb) and $^5D_4$(Tb) levels to the $^3(\pi\pi^*)$ state, which is nearly in resonance with the latter.

On the other hand, no Ln(III) emission has been detected upon ligand excitation for the Eu(III), Nd(III), Gd(III), and Ho(III) complexes. The case of the Eu(III) complexes has already been discussed. The Nd(III) ion is known to have a very low quantum efficiency in organic macromolecular complexes because of effective phonon deactivation. The Gd(III) ion has ^6P excited states at higher energy than the $^1(\pi\pi^*)$ level of the ligand so that no energy-transfer process takes place. In Ho(III) crystalline complexes, one evidences a radiative energy-transfer process. The $^5G_6 \leftarrow {}^5I_8$ and $(^5G,^3G)_5 \leftarrow {}^5I_8$ absorptions at 360 and 415 nm in the $^1(\pi\pi^*)$ ligand emission spectrum correspond to the reabsorption of photons emitted by the ligand with energy in resonance with the Ho(III) hypersensitive absorption transitions (Figure S5, supplementary material). No ligand emission is observed in Gd(III) complexes, probably because of the effect of the strong paramagnetism of this ion on the $^1(\pi\pi^*)$ state.[35] The Ho(III) complexes also display evidence of a paramagnetic $^1(\pi\pi^*)$-quenching. The ligand emission of the latter is weak by comparison with the ligand emission of the less paramagnetic Yb(III) complexes.

Conclusions

The present work demonstrates the potential of lanthanide luminescence for solving structural and analytical problems. We have evidenced small variations in the crystal field potential when a Ln(III) ion is replaced by another one and between two different α and β crystalline phases. Moreover, we have shown that the low quantum efficiency of the Eu(III) emission is due to the low-lying LMCT state. The effect of the latter considerably enhances the Eu(III) f–f absorption probabilities giving rise to a very large Ω_2 value. For a quantitative interpretation, new eigenfunctions should be recalculated for Eu(III) taking into account both the LMCT state-mixing[34] and the *j*-mixing.[32]

In contrast, the high luminescence quantum yield of Tb(III) complexes upon ligand excitation is due to energy absorption by the eight arene units of the macrocycle, followed by an efficient intramolecular energy transfer. Significant overlap is a necessary condition for an efficient energy-transfer process by an exchange mechanism and appears to be responsible for the very high energy at which the $^5D_0 \leftarrow {}^7F_0$ transition takes place. Encapsulation of the Tb(III) ion within a calixarene appears to be an effective means of obtaining a highly luminescent probe.

Acknowledgment. This work is supported through grants from the Swiss National Science Foundation. We thank the Fondation Herbette (Lausanne, Switzerland) for the gift of two lasers, Ms. Véronique Foiret for technical help, and Dr. F. Auzel (CNET, Bagneux, France) for helpful discussions.

Supplementary Material Available: One table listing transition assignments and five figures (10 pages). Ordering information is given on any current masthead page.

(36) Blasse, G.; Dirksen, G. J.; Sabbatini, N.; Perathoner, S.; Lehn, J.-M.; Alpha, B.; *J. Phys. Chem.* **1988**, *92*, 2419.